Eur. Phys. J. B **33**, 339–346 (2003)
DOI: 10.1140/epjb/e2003-00174-7

THE EUROPEAN PHYSICAL JOURNAL B

On the nature of the low-temperature phase in discontinuous mean-field spin glasses

A. Montanari[1] and F. Ricci-Tersenghi[2,a]

[1] Laboratoire de Physique Théorique de l'École Normale Supérieure[b], 24 rue Lhomond, 75231 Paris Cedex 05, France
[2] Dipartimento di Fisica and SMC and UdR1 of INFM Università di Roma "La Sapienza" Piazzale Aldo Moro 2, 00185 Roma, Italy

Received 10 February 2003
Published online 20 June 2003 –

Abstract. The low-temperature phase of discontinuous mean-field spin glasses is generally described by a one-step replica symmetry breaking (1RSB) ansatz. The Gardner transition, *i.e.* a *very*-low-temperature phase transition to a full replica symmetry breaking (FRSB) phase, is often regarded as an inessential, and somehow exotic phenomenon. In this paper we show that the metastable states which are relevant for the out-of-equilibrium dynamics of such systems are *always* in a FRSB phase. The only exceptions are (to the best of our knowledge) the p-spin spherical model and the random energy model (REM). We also discuss the consequences of our results for aging dynamics and for local search algorithms in hard combinatorial problems.

PACS. 75.50.Lk Spin glasses and other random magnets

1 Introduction and main results

During the last decade the p-spin spherical spin glass has been thoroughly investigated both in its statical and in its dynamical behavior [1–4]. In fact this model is usually considered the prototypical example of discontinuous mean-field spin glasses. The latter, in turn, have been argued to be crucial for understanding the structural glass transition [5]. In this paper we show that the p-spin spherical model is indeed quite an exceptional case among discontinuous mean-field models. While our results do not invalidate the insight gained so far, they add some new important feature to the general picture.

The out-of-equilibrium dynamics of the p-spin spherical models is closely related to the structure of metastable states [6]. Below the dynamical temperature $T_{\rm d}$, the Gibbs measure decomposes among an exponential number of metastable states, whose free-energy densities lie between two values $f_{\rm s}$ and $f_{\rm d}$. The relevant quantity in this regime is the complexity (or configurational entropy) $\Sigma_T(f)$. This is defined in terms of the number $\mathcal{N}_T(f)$ of metastable states having free energy density f,

$$\mathcal{N}_T(f) \sim \exp\{N\Sigma_T(f)\}, \tag{1}$$

N being the number of degrees of freedom of the system. $\Sigma_T(f)$ is strictly positive between $f_{\rm s}$ and $f_{\rm d}$, with an absolute maximum at $f_{\rm d}$. The free-energy density $f_*(T)$ of the pure states which dominate the Gibbs measure, results from the balance between energetic and entropic considerations. While the former would privilege the states at $f_{\rm s}$, the latter favor the states at $f_{\rm d}$.

On the other hand, in a typical out-of-equilibrium set up, the system is rapidly cooled below $T_{\rm d}$ from its high-temperature phase [3]. In the thermodynamic limit, the system never equilibrates and its behavior is dominated by the most numerous metastable states, *i.e.* the ones at $f_{\rm d}$. This means that, for any single-time observable $\mathcal{O}(t)$, the following identity holds

$$\lim_{t\to\infty}\lim_{N\to\infty}\langle\mathcal{O}(t)\rangle = \lim_{N\to\infty}\langle\mathcal{O}\rangle_{f_{\rm d}}, \tag{2}$$

where the average on the left-hand side is taken with respect to thermal histories, while on the right-hand side it is taken with respect to a constrained Gibbs measure. Outside the thermodynamic limit, the system eventually equilibrates on an exponential time scale $t_{\rm erg}(N) = \exp\{O(N)\}$.

The complexity $\Sigma_T(f)$ can be calculated within a 1RSB scheme [7]. This calculation is known to be correct for the p-spin spherical model [1]. This does not rule out the possibility of further replica-symmetry breakings for more general cases: one would then expect a FRSB calculation to be necessary. The consequences of FRSB on the above picture have not been investigated so far. However, it is usually thought that FRSB would play a minor role. The intuition, as far as we can understand it, goes as

[a] e-mail: Federico.Ricci@roma1.infn.it
[b] UMR 8549, Unité Mixte de Recherche du Centre National de la Recherche Scientifique et de l' École Normale Supérieure

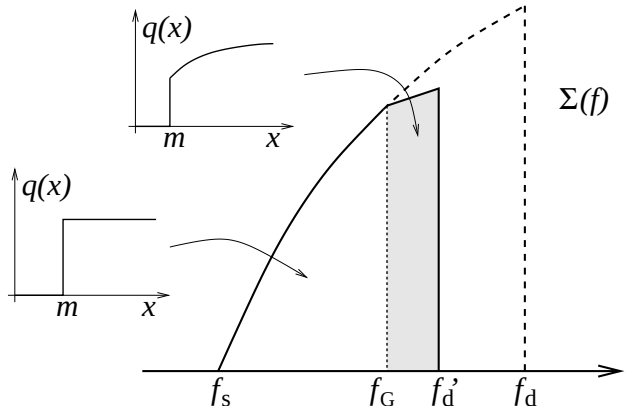

Fig. 1. The complexity curve for a generic discontinuous mean-field spin glass. The dashed line is the 1RSB approximation, while the continuous line is the exact result. The two coincide below f_G. The gray region is FRSB. The shape of the Parisi order parameter is shown in the insets.

follows. As shown in 1985 by Elisabeth Gardner [8] in the case of the p-spin Ising model, discontinuous spin glasses may have a FRSB phase which overcomes the 1RSB phase at *very* low temperature. The common wisdom associates low temperature to low energy: if any FRSB effect is present, it affects, at most, the lowest part of the complexity spectrum. As a consequence, out-of-equilibrium dynamics is unaffected by FRSB. Here we show that this intuition is incorrect and that FRSB plays an important role also for discontinuous mean-field glasses.

The correct scenario is sketched in Figure 1. The 1RSB solution is stable with respect to FRSB up to some value f_G of the free-energy density. At higher free energies, the 1RSB solution becomes unstable and a FRSB calculation is required. Quite generally $f_G < f_d$ strictly. We know just two exceptions to this rule (both are somehow degenerate cases): the spherical model and the REM [9]. On the contrary both the situations $f_G < f_s$ and $f_G > f_s$ are possible. A thermodynamic FRSB phase transition occurs when f_G crosses $f_*(T)$. Above f_G, the FRSB calculation will give a new complexity curve, and, in particular a new threshold free energy f_d'. Of course, out-of-equilibrium dynamics will be dominated (in the sense of Eq. (2)) by the states at f_d'. Of course, the nature of aging dynamics will change. We expect relaxation to be characterized by an infinite number of time sectors [10,11] (instead of just two), although two of them will be most relevant (namely the first and the last one).

In the next sections we shall illustrate the general scenario with two examples which are, at the same time, simple and representative. In Section 2 we reconsider the fully-connected Ising p-spin model. Let us mention that the marginality point f_G has been already computed for a fully-connected model [13]. Nevertheless, its relation with the complexity curve, *cf.* Figure 1, has never been elucidated. In Section 3 we turn to finite-connectivity models at zero temperature. In this case we can compare our results with numerical simulations.

2 Infinite connectivity

The fully-connected p-spin model is defined by the Hamiltonian

$$\mathcal{H}(\sigma) = -\sum_{(i_1 \dots i_p)} J_{i_1 i_2 \dots i_p} \sigma_{i_1} \sigma_{i_2} \dots \sigma_{i_p} \quad , \tag{3}$$

where the N variables $\sigma_i = \pm 1$ are Ising spins and the $J_{i_1 i_2 \dots i_p}$ are quenched random interactions extracted from a Gaussian distribution with zero mean and variance $p!/(2N^{p-1})$. For illustration we shall often consider the $p = 3$ case, although our results are qualitatively valid for any finite $p > 2$.

Using the standard replica formalism with a 1RSB ansatz, one obtains the action [8]

$$\phi(\beta, m) = -\frac{\beta}{4}\left[1 + (p-1)(1-m)q^p - p\,q^{p-1}\right] - \frac{1}{\beta}\log 2 - \frac{1}{\beta m}\log \int \mathcal{D}z\, \cosh^m(\beta\lambda\, z)\,, \tag{4}$$

where $\mathcal{D}z \equiv \mathrm{e}^{-z^2/2}\,\mathrm{d}z/\sqrt{2\pi}$, $\lambda \equiv \sqrt{\frac{p}{2}\,q^{p-1}}$ and q is determined by the saddle point equation

$$q = \frac{\int \mathcal{D}z\, \cosh^m(\beta\lambda z) \tanh^2(\beta\lambda z)}{\int \mathcal{D}z\, \cosh^m(\beta\lambda z)}. \tag{5}$$

From the action (4) we have the usual parametric representation [7] of the complexity $\Sigma_T(f)$ at temperature $T = 1/\beta$:

$$\Sigma = \beta m^2 \partial_m \phi(\beta, m)\,, \qquad f = \partial_m[m\,\phi(\beta, m)]\,. \tag{6}$$

The outcome of these formulae agrees with the general picture sketched in Figure 1, that is $\Sigma_T(f)$ is positive for $f \in [f_s, f_d]$, which corresponds to $m \in [m_s, m_d]$. Both the extrema of this range depend on the temperature. The internal energy of metastable states can be calculated using the identity

$$e(\beta, m) = -\frac{1}{N}\sum_{(i_1,\dots,i_p)} \overline{J_{i_1 i_2 \dots i_p} \langle \sigma_{i_1} \sigma_{i_2} \dots \sigma_{i_p} \rangle} = -\frac{\beta}{2}\Big[1 - (1-m)\,q^p\Big], \tag{7}$$

where q satisfies equation (5).

The thermodynamics of the model at temperature T (within the 1RSB approximation) is obtained maximizing $\phi(T, m)$ with respect to $m \in [0, 1]$. The resulting $m_s(T)$ is shown in Figure 2 (dotted-dashed curve): it becomes smaller than 1 at the critical temperature T_s and

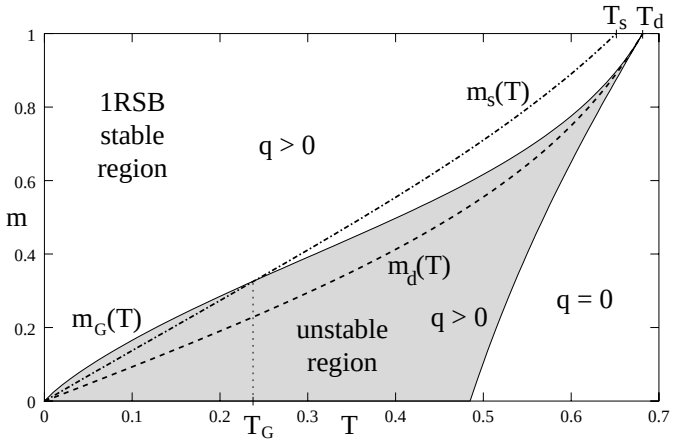

Fig. 2. 3-spin fully-connected Ising model: the Parisi parameter m for thermodynamic states (dotted-dashed curve) and for threshold states (dashed curve) as a function of the temperature. In the shaded region, 1RSB solutions are unstable with respect to further replica symmetry breakings.

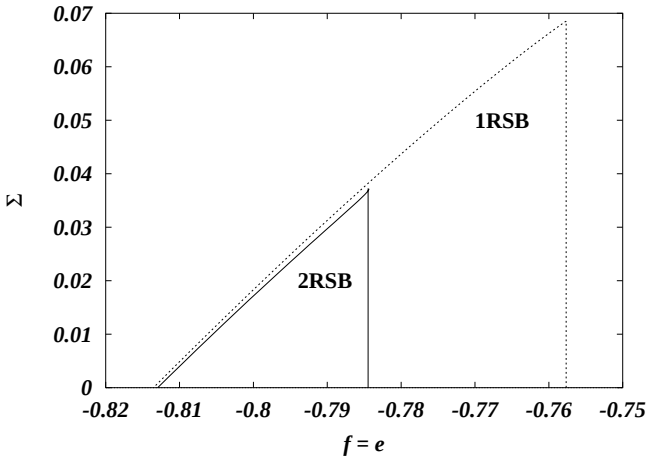

Fig. 3. $T = 0$ complexity as a function of the (free) energy density for the 3-spin fully-connected Ising model, obtained with 1RSB and 2RSB approximations.

it vanishes for $T \to 0$ as $m_{\rm s} \sim \mu_{\rm s} T$. Threshold states, those maximizing the complexity Σ, are obtained fixing $m = m_{\rm d}(T)$, which is shown in Figure 2 with a dashed curve: $m_{\rm d}(T)$ becomes smaller than 1 at the dynamical critical point $T_{\rm d}$ and vanishes as $m_{\rm d} \sim \mu_{\rm d} T$.

The stability of the 1RSB solution with respect to a second step (and eventually infinite steps) of replica symmetry breaking can be evaluated following reference [8]. For any given T and m the 1RSB solution is stable provided

$$\frac{2}{p(p-1)\beta^2 q^{p-2}} > \frac{\int \mathcal{D}z\, \cosh^{m-4}(\beta\lambda z)}{\int \mathcal{D}z \cosh^{m}(\beta\lambda z)}. \qquad (8)$$

In Figure 2 the region where replica symmetry should be broken more than once has been shaded. We call $m_{\rm G}(T)$ its boundary. In reference [8] Elizabeth Gardner calculated the critical point $T_{\rm G}$ where thermodynamic states are no longer 1RSB (this point was called T_2 in Ref. [8]). Still more interesting is the fact that *threshold states are always in the unstable region.*

The physical scenario already described in Section 1 (see Fig. 1) is confirmed for any temperature below $T_{\rm d}$. In general we find that $f_{\rm G}$ is strictly less than $f_{\rm d}$, while both the inequalities $f_{\rm G} < f_{\rm s}$ and $f_{\rm G} > f_{\rm s}$ are possible, depending on the temperature. For $f < f_{\rm G}$ the 1RSB solution is correct and the Parisi order parameter $q(x)$ has a single step at $x = m$ (see lower inset in Fig. 1 and please remind that in the absence of an external field $q_0 = 0$). For $f > f_{\rm G}$, the FRSB calculation will give an order parameter $q(x)$ with a continuous non-trivial part above the step (see upper inset in Fig. 1), a new complexity curve and, in particular, a new threshold free energy $f'_{\rm d}$. The geometrical structure of metastable states above $f_{\rm G}$ is therefore the following. There is an exponential number of *families* of states, each one having a FRSB structure inside. The typical overlap between two families is 0, while the minimum overlap between states of the same family is given by the step size in the function $q(x)$.

Let us suggest a natural generalization of the above method, for computing $\Sigma(f)$ above $f_{\rm G}$. Given the free-energy functional [12] $\Phi_{\rm FRSB}[T, q(x)]$, one can parameterize $q(x)$ by the jump location m and by the continuous function $r(x)$ for $x \in [m, 1]$. Then one can define $\phi(T, m) = \max_{r(x)} \Phi_{\rm FRSB}[T, q(x)]$, by maximizing the free-energy functional for fixed T and m[1]. Finally the complexity is obtained by taking the Legendre transform of $\phi(T, m)$ as in equation (6). The complete calculation can be done using *e.g.* the numerical method of reference [14]. Here we show the result of a 2RSB approximated calculation at zero temperature.

In the $T \to 0$ limit, the 1RSB free energy is simply given by

$$\phi^{\rm 1RSB}_{T=0}(\mu) = -\frac{\mu}{4} - \frac{1}{\mu} \ln \left[1 + {\rm erf}\left(\frac{\sqrt{p}}{2} \mu \right) \right] \quad , \qquad (9)$$

where $\mu = \lim_{\beta\to\infty} \beta m$ and ${\rm erf}(x) \equiv 2 \int_0^x {\rm d}t\, {\rm e}^{-t^2}/\sqrt{\pi}$. The resulting complexity $\Sigma(e)$ is shown in Figure 3 (dashed curve).

The 2RSB free energy $\phi^{\rm 2RSB}_{T=0}(\mu_1, \mu_2)$ depends on two numbers which parameterize, as in the 1RSB case, the zero temperature limit of the Parisi breaking parameters. The three overlaps behaves as follows: $q_0 = 0$, $q_1 = q$ (with $0 < q < 1$ strictly) and $q_2 \simeq 1 - \omega T$. The saddle point

[1] This means that one has to maximize $\Phi_{\rm FRSB}[T, q(x)]$ among all the order parameters $q(x)$ such that $q(x) = 0$ for $x < m$. Let us call $m_{\rm s}^{\rm FRSB}$ the position of the discontinuity in the statical FRSB solution $q_{\rm s}(x)$. If $m < m_{\rm s}^{\rm FRSB}$, there is one trivial solution to this maximization problem: $q(x) = q_{\rm s}(x)$. We expect a non-trivial secondary maximum to exist. On such a maximum the discontinuity in $q(x)$ is located at m. This expectation is indeed confirmed by our 2RSB calculation.

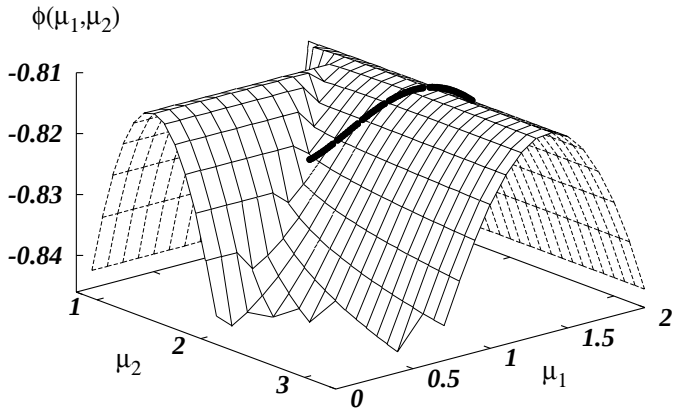

Fig. 4. Replicated free-energy for the 3-spin fully-connected Ising model at $T = 0$ as a function of the breaking parameters. The bold line is the result of a maximization over μ_2 at fixed μ_1. It ends on the border of the region with $q = 0$ (left paraboloid). Notice that the trivial maximum in this region has to be discarded when computing the complexity, since it has $\partial_{\mu_1}\phi(\mu_1, \mu_2) = 0$.

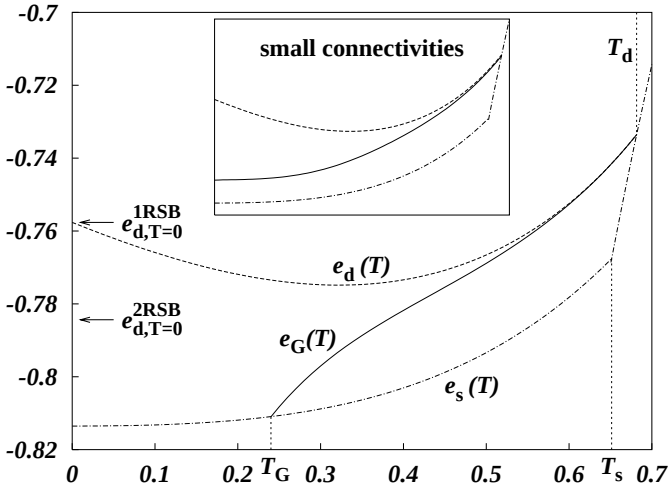

Fig. 5. Thermodynamic energy (dotted-dashed line) and threshold energy (dashed line) as a function of the temperature within the 1RSB approximation. States above the full line are unstable with respect to further replica symmetry breakings. The arrows mark the threshold energies calculated directly at $T = 0$. Main panel: 3-spin fully-connected Ising model. Inset: pictorial view for a 3-spin with small connectivity.

equation for q reads

$$q = \frac{\int \mathcal{D}z\; I_+^{\nu-2}(z,q,\mu_2)\; I_-^2(z,q,\mu_2)}{\int \mathcal{D}z\; I_+^{\nu}(z,q,\mu_2)}, \qquad (10)$$

$$I_\pm(z,q,\mu_2) = \frac{\mathrm{e}^{\mu_2\lambda z}}{2}\left[1+\mathrm{erf}\left(\frac{\eta\mu_2}{2}+\frac{\lambda z}{\eta}\right)\right] \pm \frac{\mathrm{e}^{-\mu_2\lambda z}}{2}\left[1+\mathrm{erf}\left(\frac{\eta\mu_2}{2}-\frac{\lambda z}{\eta}\right)\right], \qquad (11)$$

where $\nu \equiv \mu_1/\mu_2$, $\lambda \equiv \sqrt{\frac{p}{2}\,q^{p-1}}$ and $\eta \equiv \sqrt{p(1-q^{p-1})}$. At the saddle point, the expressions for the action and the energy simplify to

$$\phi(\mu_1,\mu_2) = -\frac{\mu_2}{4}\Big[1+(p-1)(1-\nu)q^p - p\,q^{p-1}\Big] - \frac{1}{\mu_1}\ln\int \mathcal{D}z\; I_+^{\nu}(z,q,\mu_2), \qquad (12)$$

$$e(\mu_1,\mu_2) = -\frac{1}{2}\Big[p\,\omega(q,\mu_2) + \mu_2 - (\mu_2-\mu_1)q^p\Big], \qquad (13)$$

$$\omega(q,\mu_2) = \frac{2}{\sqrt{\pi p}}\mathrm{e}^{-\frac{1}{4}\nu^2\mu_2^2}\frac{\int \mathcal{D}z\; I_+^{\nu-1}(z\sqrt{1-q^{p-1}},q,\mu_2)}{\int \mathcal{D}z\; I_+^{\nu}(z,q,\mu_2)}, \qquad (14)$$

where, as usual, q satisfies the saddle point equation (10). In the interesting region of parameters the shape of $\phi(\mu_1, \mu_2)$ is that of 2 com-penetrating paraboloids (see Fig. 4): On the left paraboloid we have that $q = 0$ and we recover the 1RSB solution with $\mu = \mu_2$, while on the right paraboloid q takes non-trivial values and we find there the absolute maximum of $\phi(\mu_1, \mu_2)$, corresponding to the ground state energy. Please note that, on the right paraboloid, the most relevant variable is the smaller breaking parameter μ_1.

We proceed by maximizing $\phi(\mu_1, \mu_2)$ over μ_2, and Legendre-transforming the result with respect to μ_1. The result is shown in Figure 3 (continuous line). It is worth mentioning at least two important facts:

- The 2RSB threshold energy $e_{\mathrm{d}}^{\mathrm{2RSB}}$ is much lower than the 1RSB one $e_{\mathrm{d}}^{\mathrm{1RSB}}$.
- In the region between e_s^{2RSB} and e_d^{2RSB} the complexity curve does not change significantly. In general we expect $\Sigma(e)$ not to change below e_{G}, but in this case $e_{\mathrm{G}} < e_{\mathrm{s}}^{\mathrm{2RSB}}$.

How does this new physical scenario affect observable quantities, like the internal energy? In the main panel of Figure 5 we plot the thermodynamic energy $e_{\mathrm{s}}(T)$, the threshold states energy $e_{\mathrm{d}}(T)$, and the internal energy $e_{\mathrm{G}}(T)$ at the instability point, for the fully-connected 3-spin model. The incorrectness of the 1RSB ansatz for threshold states is clear from the unphysical behavior of $e_{\mathrm{d}}(T)$, which is not a monotonously increasing function of T: an annealing experiment at temperature T, would produce, accordingly to equation (2), a larger asymptotic energy when temperature is decreased!

Let us imagine to cool down rapidly the system at some temperature $T < T_{\mathrm{d}}$, and watch its internal energy density $e_T(t)$. The asymptotic energy $e_T(\infty)$ must lie below $e_{\mathrm{d}}(T)$ and above both $e_{\mathrm{s}}(T)$ and $e_{\mathrm{G}}(T)$, and it must be a monotonously increasing function of T. We can estimate $e_{\mathrm{d}}(T = 0)$, from the zero-temperature 2RSB calculation above. The result is marked by an arrow in Figure 5. As already noticed, this value is much lower than what predicted by an 1RSB calculations. An even smaller internal energy can be obtained by an extremely slow cooling [15]. Such a conclusion has positive consequences on the use of simulated annealing and related techniques for the search of low energy solutions in hard combinatorial problems.

However, the situation is not always like the one just described. In some cases, $e_{\mathrm{G}}(T) > e_{\mathrm{s}}(T)$ for all

temperatures below $T_{\rm d}$ (see the sketch in the inset of Fig. 5). This is what actually happens for p-spin models with small connectivities, as will be shown in the next section.

3 Finite connectivity and numerical simulations

Finite connectivity mean-field models have been the object of intense investigation in the last years. On one hand, they are thought to share some properties of finite-dimensional models (namely each spin interact with a finite number of neighbors). On the other hand, they are closely related to extremely hard combinatorial optimization problems [16]. Nevertheless, up to now, the theoretical investigations have been limited to the 1RSB level [17,18]. Here we want to show how the 1RSB phase becomes unstable with respect to 2RSB fluctuations, and how to compute the stability threshold. We expect that, as usual, once the 1RSB phase becomes unstable, FRSB has to be used for properly describing the system.

For sake of simplicity, we present our calculation in a particularly simple case, which allows a fully explicit derivation. We shall comment later on the generalizations of our results. To be definite, let us consider a fixed-connectivity Ising model with p-spin interactions (hereafter $p > 2$) with Hamiltonian

$$\mathcal{H}(\sigma) = -\sum_{(i_1\dots i_p)\in\mathcal{G}} J_{i_1\dots i_p}\sigma_{i_1}\dots\sigma_{i_p}. \qquad (15)$$

In the above formula $\mathcal{G}$ is the hypergraph of interactions, *i.e.* a set of M among the $\binom{N}{p}$ possible p-uples of the N spins. Here we shall take $\mathcal{G}$ to have fixed connectivity: each spin is supposed to participate to $(l+1)$ interaction terms. Finally we shall consider the couplings $J_{i_1\dots i_p}$ to take the values ± 1 with equal probability.

Under these hypothesis the 2RSB order parameter is a normalized measure on a space of probability distributions and does not depend upon the site of the sample [19]. The mean-field equations are most conveniently written in terms of two such measures: $\mathcal{Q}[\underline{\rho}]$ and $\widehat{\mathcal{Q}}[\underline{\widehat{\rho}}]$. At zero temperature they have the form

$$\mathcal{Q}[\underline{\rho}] = \frac{1}{\mathcal{Z}}\int\prod_{\alpha=1}^{l} d\widehat{\mathcal{Q}}\left[\underline{\widehat{\rho}}^{(\alpha)}\right]\; z\left[\left\{\underline{\widehat{\rho}}^{(\alpha)}\right\}\right]^{\mu_1/\mu_2}\delta\left[\underline{\rho}-\underline{\rho}^{(0)}\left[\left\{\underline{\widehat{\rho}}^{(\alpha)}\right\}\right]\right], \qquad (16)$$

$$\widehat{\mathcal{Q}}[\underline{\widehat{\rho}}] = \int\prod_{i=1}^{p-1} d\mathcal{Q}\left[\underline{\rho}^{(i)}\right]\;\delta\left[\underline{\widehat{\rho}}-\underline{\widehat{\rho}}^{(0)}\left[\left\{\underline{\rho}^{(i)}\right\}\right]\right], \qquad (17)$$

where $\mathcal{Z}$ is a normalization constant and $0 < \mu_1 \le \mu_2 < \infty$ are the 2RSB parameters in the $\beta\to\infty$ limit. The probability distribution $\widehat{\underline{\rho}}$ is supported over the integers q such that $-1 \le q \le +1$. It is therefore given in terms of three positive numbers: $\widehat{\underline{\rho}} = \{\widehat{\rho}_+, \widehat{\rho}_0, \widehat{\rho}_-\}$ (with $\widehat{\rho}_+ + \widehat{\rho}_0 + \widehat{\rho}_- = 1$). The distribution $\underline{\rho}$ is instead supported over the integers $-l \le q \le l$. However, for our purposes, we can parametrize it using the three numbers $\{\rho_+ \equiv \sum_{q=1}^{l}\rho_q, \rho_0, \rho_- = \sum_{q=-l}^{-1}\rho_q\}$. The "functionals" $\mathcal{Q}[\underline{\rho}]$ and $\widehat{\mathcal{Q}}[\underline{\widehat{\rho}}]$ are therefore nothing but distributions over two-dimensional simplexes. Finally, the functions $\underline{\rho}^{(0)}[\dots]$ and $\underline{\widehat{\rho}}^{(0)}[\dots]$ entering in equations (16–17) are defined as follows:

$$\rho^{(0)}_{+,0,-} = \frac{1}{z\left[\left\{\underline{\widehat{\rho}}^{(\alpha)}\right\}\right]} \times \sum_{\substack{\{q_\alpha\}\\ \sum q_\alpha >0,=0,<0}}\prod_{\alpha=1}^{l}\widehat{\rho}^{(\alpha)}_{q_i}\,\exp\left\{-\mu_2\left[\sum_{\alpha=1}^{l}|q_i| - |\sum_{\alpha=1}^{l} q_i|\right]\right\}, \qquad (18)$$

$$\widehat{\rho}^{(0)}_q = \begin{cases} \frac{1}{2}\left[\prod_{i=1}^{p-1}\left(\rho^{(i)}_+ + \rho^{(i)}_-\right) + \prod_{i=1}^{p-1}\left(\rho^{(i)}_+ - \rho^{(i)}_-\right)\right] & \text{if } q = +\,, \\ 1 - \prod_{i=1}^{p-1}\left(\rho^{(i)}_+ + \rho^{(i)}_-\right) & \text{if } q = 0\,, \\ \frac{1}{2}\left[\prod_{i=1}^{p-1}\left(\rho^{(i)}_+ + \rho^{(i)}_-\right) - \prod_{i=1}^{p-1}\left(\rho^{(i)}_+ - \rho^{(i)}_-\right)\right] & \text{if } q = -, \end{cases} \qquad (19)$$

and the constant $z[\{\underline{\widehat{\rho}}^{(\alpha)}\}]$ is such that $\underline{\rho}^{(0)}$ is normalized.

The authors of reference [19] considered the 1RSB solution to this problem. This is nothing but the fixed point $(\underline{\rho}^*, \underline{\widehat{\rho}}^*)$ of equations (18, 19):

$$\underline{\rho}^* = \underline{\rho}^{(0)}[\underline{\widehat{\rho}}^*, \dots, \underline{\widehat{\rho}}^*]\,; \quad \underline{\widehat{\rho}}^* = \underline{\widehat{\rho}}^{(0)}[\underline{\rho}^*, \dots, \underline{\rho}^*]\,. \qquad (20)$$

The above equations have always a symmetric solution: $\rho^*_+ = \rho^*_-$, $\widehat{\rho}^*_+ = \widehat{\rho}^*_-$, which is the physical one. The physical stability of the 1RSB phase coincides with the stability of this solution under the iteration (16–17). We must therefore consider how the 2RSB order parameters $\mathcal{Q}[\underline{\rho}]$, $\widehat{\mathcal{Q}}[\underline{\widehat{\rho}}]$ can reduce to the 1RSB solution (20):

- The first possibility is that $\mathcal{Q}[\underline{\rho}]$ and $\widehat{\mathcal{Q}}[\underline{\widehat{\rho}}]$ concentrate around $\underline{\rho}^*$, $\underline{\widehat{\rho}}^*$:

$$\mathcal{Q}[\underline{\rho}] \approx f(\underline{\rho} - \underline{\rho}^*)\,, \quad \widehat{\mathcal{Q}}[\underline{\widehat{\rho}}] \approx \widehat{f}(\underline{\widehat{\rho}} - \underline{\widehat{\rho}}^*), \qquad (21)$$

  where $f(\cdot)$ and $\widehat{f}(\cdot)$ are supported in a neighborhood of $\underline{0}$. The two distributions on the two-dimensional simplex $\mathcal{Q}$, $\widehat{\mathcal{Q}}$ tend, in the 1RSB limit, to delta functions in a particular point $(\underline{\rho}^*, \underline{\widehat{\rho}}^*)$ of the simplex.
  The stability condition of the delta-function solution under perturbations of the type (21) is easily derived. Define the 2×2 matrices L and $\widehat{L}$ by linearizing

equations (18, 19) around $(\underline{\rho}^*, \underline{\widehat{\rho}}^*)$:

$$L_{q,q'} = \left.\frac{\partial \rho_q^{(0)}}{\partial \widehat{\rho}_{q'}^{(1)}}\right|_{\underline{\rho}^*}, \qquad \widehat{L}_{q,q'} = \left.\frac{\partial \widehat{\rho}_q^{(0)}}{\partial \rho_{q'}^{(1)}}\right|_{\underline{\widehat{\rho}}^*}, \quad \text{for } q, q' \in \{+,-\}. \quad (22)$$

If we call $\lambda_{\rm MAX}$ the eigenvalue of their product $L \cdot \widehat{L}$ having the maximum absolute value, we obtain the stability condition

$$l(p-1) \cdot |\lambda_{\rm MAX}|^2 < 1\,. \quad (23)$$

In fact the matrices L and $\widehat{L}$ can be easily diagonalized by using symmetry considerations: one of the two eigenvectors is symmetric, and the other is antisymmetric under the exchange $+ \leftrightarrow -$. The antisymmetric eigenvalue vanishes for $p > 2$. The symmetric one can be shown to verify always the stability condition (23). This type of instability is therefore irrelevant for the problem under study.

- The second possibility is that the functionals $\mathcal{Q}[\underline{\rho}]$ and $\widehat{\mathcal{Q}}[\underline{\widehat{\rho}}]$ concentrate around delta-function distributions:

$$\mathcal{Q}[\underline{\rho}] \approx \rho_+^* f_+[\underline{\rho} - \underline{\delta}_+] + \rho_0^* f_0[\underline{\rho} - \underline{\delta}_0] + \rho_-^* f_-[\underline{\rho} - \underline{\delta}_-], \quad (24)$$

and analogously for $\widehat{\mathcal{Q}}[\underline{\widehat{\rho}}]$. In the above expression the distributions $f_q[\cdot]$ are supported around $\underline{0}$, and $\underline{\delta}_+$ (respectively $\underline{\delta}_0$, $\underline{\delta}_-$) is the distribution $\{1,0,0\}$ (respectively $\{0,1,0\}$, $\{0,0,1\}$). In other words the measures $\mathcal{Q}[\underline{\rho}]$ and $\widehat{\mathcal{Q}}[\underline{\widehat{\rho}}]$ concentrate over the corners of the simplex, with weights given by the 1RSB solution.
In order to derive the stability condition it is convenient to use variables which are small near the corners of the simplex. One possible choice is to rewrite the distributions $f_q[\cdot]$ as functions of the variables

$$\epsilon_\pm = \rho_\pm - \delta_{q,\pm}\,, \quad (25)$$

and analogously for the distributions $\widehat{f}_q[\cdot]$. Notice that two variables are sufficient because of the normalization constraint. Moreover the signs of ϵ_+, ϵ_- are fixed by the value of q. It is now easy to linearize the equations for $f_q[\cdot]$, $\widehat{f}_q[\cdot]$ in the limit $\epsilon_\pm \ll 1$. If we define $\langle \epsilon_\pm \rangle_q$ (respectively $\langle \widehat{\epsilon}_\pm \rangle_{\widehat{q}}$), the average of $\epsilon_\pm$ ($\widehat{\epsilon}_\pm$) with respect to $f_q[\cdot]$ ($\widehat{f}_{\widehat{q}}[\cdot]$), we get the equations

$$\langle \epsilon_\sigma \rangle_q \approx l \sum_{\widehat{q},\widehat{\sigma}} T_{q\sigma,\widehat{q}\widehat{\sigma}} \langle \widehat{\epsilon}_{\widehat{\sigma}} \rangle_{\widehat{q}},$$
$$\langle \widehat{\epsilon}_{\widehat{\sigma}} \rangle_{\widehat{q}} \approx (p-1) \sum_{q,\sigma} \widehat{T}_{\widehat{q}\widehat{\sigma},q\sigma} \langle \epsilon_\sigma \rangle_q, \quad (26)$$

where the sums over q and $\widehat{q}$ run over $\{+,0,-\}$, while the ones over σ and $\widehat{\sigma}$ run over $\{+,-\}$. Explicit formulae for the 6×6 matrices T and $\widehat{T}$ are reported in Appendix A. As before, we look for the eigenvalue of the product $T \cdot \widehat{T}$ which has the largest absolute value. If we call $\omega_{\rm MAX}$ this eigenvalue, the stability criterion is

$$l(p-1) \cdot |\omega_{\rm MAX}| < 1. \quad (27)$$

It turns out that $\omega_{\rm MAX}$ depends uniquely on the parameter μ_1, which can be identified as the 1RSB parameter. This criterion, unlike (23), has a non-trivial content which we shall consider in the following.

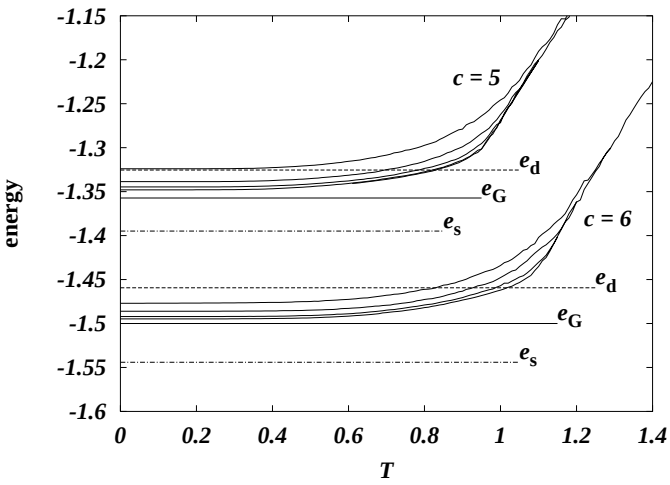

Fig. 6. 3-spin Ising model with fixed connectivity c, energy relaxation during slow simulated annealings. The 4 different full curves correspond to 4 cooling rates proportional to 1, 10^{-1}, 10^{-2}, 10^{-3}. The values for $e_{\rm d}$, $e_{\rm G}$ and $e_{\rm s}$ are those reported in Table 1.

The criterion (27) select a range of the 1RSB parameter for which the 1RSB solution is stable. This range has the form $\mu > \mu_{\rm G}$. Using the relation between μ and the energy e of metastable states [7], see also the previous section, one can convert this condition as an energy condition of the form $e < e_{\rm G}$. This confirms our general picture summarized in Figure 1.

In Table 1 we exemplify the general situation by considering the case $p = 3$. In the low connectivity regime $(l+1) \leq 10$ we have $e_{\rm s} < e_{\rm G} < e_{\rm d}$ strictly: the ground state is correctly described by 1RSB while high-lying metastable states are unstable to FRSB. The expected temperature dependence of $e_{\rm d}$ in this regime of connectivities, is sketched in the inset of Figure 5. At higher connectivities the ground state becomes unstable too: $e_{\rm G} < e_{\rm s} < e_{\rm d}$. We know that the last situation is verified in the infinite-connectivity limit, *cf.* Section 2. Moreover, for even connectivities, the instability point corresponds to the vanishing of the 0-component of the 1RSB parameter $\widehat{\rho}_0^*$, and thus the ground state become unstable when $\widehat{\rho}_0^*(\mu_{\rm s})$ becomes positive.

For $(l+1) \leq 10$, we are in the case depicted in the inset of Figure 5, since the instability energy $e_{\rm G}$ lies above the ground state energy $e_{\rm s}$. In this situation there is a lower bound on the energy reachable by simulated annealing (and presumably by any local search algorithm running in a time polynomial in N) which is strictly above the ground state energy, and the problem of finding the ground state is hard and not approximable [20].

Table 1. 3-spin with fixed connectivity $(l+1)$ at $T = 0$ within the 1RSB approximation: columns from 2 to 7, breaking parameter and energy corresponding to threshold (d), thermodynamic (s) and marginally-stable (G) states; column 8, 0-component of the 1RSB parameter on the states dominating the thermodynamics.

$(l+1)$	$\mu_{\rm d}$	$-e_{\rm d}$	$\mu_{\rm s}$	$-e_{\rm s}$	$\mu_{\rm G}$	$-e_{\rm G}$	$\widehat{\rho}_0^*(\mu_{\rm s})$
3	1.42832	0.958659	∞	1.0	1.70267	0.963594	0
4	0.915569	1.15267	1.4115	1.21771	1.09861	1.16667	0
5	0.716089	1.3254	1.09566	1.39492	0.958971	1.35728	0.0420615
6	0.613587	1.45936	0.901568	1.54414	0.804719	1.5	0
7	0.535146	1.59825	0.802528	1.68623	0.75739	1.66103	0.0427
8	0.49023	1.70826	0.717919	1.8092	0.677627	1.77828	0
9	0.445068	1.8279	0.663636	1.93191	0.652821	1.92257	0.0397177
10	0.41937	1.924	0.61494	2.03932	0.601444	2.02455	0
11	0.389004	2.03054	0.578677	2.14895	0.585751	2.15734	0.0366356
12	0.372092	2.11725	0.54668	2.2457	0.548851	2.2488	0.00075104
13	0.34986	2.21409	0.51988	2.34567	0.537826	2.37296	0.0339348
14	0.337728	2.2939	0.497043	2.43451	0.509535	2.4566	0.00375363
15	0.320558	2.38318	0.476086	2.52697	0.501257	2.5739	0.0316323
16	0.311329	2.45761	0.458822	2.60963	0.4786	2.65142	0.00579464
17	0.297566	2.54079	0.441831	2.696	0.472092	2.7631	0.0296691
18	0.290241	2.61089	0.428229	2.77367	0.453371	2.83566	0.00720516
19	0.278903	2.689	0.414083	2.855	0.44808	2.94261	0.0279824
20	0.272901	2.75551	0.40303	2.9285	0.432245	3.01104	0.00820489

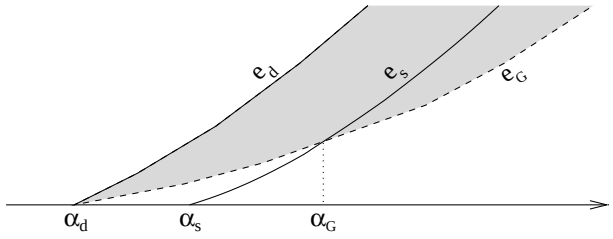

Fig. 7. The 1RSB zero-temperature phase diagram for spin models with Poissonian connectivity. The shaded area is an educated guess for range of parameter in which FRSB is needed.

We have verified this prediction by running long simulated annealings on a large instance of the 3-spin model with fixed connectivities 5 and 6. The results are shown in Figure 6, different curves corresponding to different cooling rates. For both connectivities, the energies reachable by simulated annealing are clearly below the threshold energy $e_{\rm d}$ predicted with the 1RSB ansatz. Moreover the extrapolations to infinitely slow cooling rates are perfectly compatible with the energy $e_{\rm G}$, thus suggesting that the complexity coming from the FRSB solution at $x > m$, *cf.* Figure 1, should be tiny.

Any fixed-connectivity p-spin Ising model is therefore FRSB for what concerns dynamic states. Another interesting class of diluted mean-field models consists of models defined on random hypergraphs with Poissonian connectivity. Among the others, this class includes the diluted p-spin model [21–23], also known as random p-XORSAT in theoretical computer science. The zero-temperature phase diagram for this model in 1RSB approximation is sketched in Figure 7 (we recall that in p-XORSAT energies are always positive defined). Glassy metastable states develop above the average connectivity $\alpha_{\rm d}$ and have energy densities between $e_{\rm s}(\alpha)$ and $e_{\rm d}(\alpha)$. The ground state energy $e_{\rm s}(\alpha)$ becomes positive at $\alpha_{\rm s}$ ($> \alpha_{\rm d}$). Since zero-energy configurations have been rigorously shown to possess a 1RSB structure [22,23], a quite natural conjecture for the energy above which FRSB sets in, $e_{\rm G}(\alpha)$, is reported with a dashed line. We have $e_{\rm s} < e_{\rm G} < e_{\rm d}$ for $\alpha_{\rm d} < \alpha < \alpha_{\rm G}$, and $e_{\rm G} < e_{\rm s} < e_{\rm d}$ for $\alpha > \alpha_G$. The calculation of the $e_{\rm G}(\alpha)$ curve will be presented in a forthcoming publication [24].

It is a pleasure to thank Marc Mézard for his interest in our work. We also acknowledge financial support from ESF program SPHINX and EEC network STIPCO.

Appendix A: Formulae for the stability matrices

In this Appendix we give explicit formulae for the matrices T and $\widehat{T}$ implicitly defined by equation (26). All these formulae are expressed in terms of the 1RSB solution, *cf.* equation (20). The form of the matrices is the following:

$$T = \begin{bmatrix} t_1 & t_2 & 0 & t_3 & 0 & 0 \\ 0 & t_1 & 0 & 0 & 0 & 0 \\ 0 & 0 & t_4 & 0 & 0 & t_5 \\ t_5 & 0 & 0 & t_4 & 0 & 0 \\ 0 & 0 & 0 & 0 & t_1 & 0 \\ 0 & 0 & t_3 & 0 & t_2 & t_1 \end{bmatrix}, \widehat{T} = \begin{bmatrix} \widehat{t}_1 & 0 & 0 & 0 & 0 & \widehat{t}_1 \\ 0 & \widehat{t}_1 & 0 & 0 & \widehat{t}_1 & 0 \\ 0 & 0 & \widehat{t}_2 & \widehat{t}_2 & 0 & 0 \\ 0 & 0 & \widehat{t}_2 & \widehat{t}_2 & 0 & 0 \\ 0 & \widehat{t}_1 & 0 & 0 & \widehat{t}_1 & 0 \\ \widehat{t}_1 & 0 & 0 & 0 & 0 & \widehat{t}_1 \end{bmatrix}, \quad (28)$$

where we ordered the entries in equation (26) as follows: $[\langle\epsilon_+\rangle_+, \langle\epsilon_-\rangle_+; \langle\epsilon_+\rangle_0, \langle\epsilon_-\rangle_0; \langle\epsilon_+\rangle_-, \langle\epsilon_-\rangle_-]$. The nonzero entries in the above matrices are given below

$$t_1 = \frac{\Omega_1^{(0)}}{Z_+} \qquad t_2 = \frac{\Omega_1^{(1)}}{Z_+} \quad t_3 = \frac{\Omega_0^{(1)}}{Z_+}$$
$$t_4 = \frac{\Omega_0^{(0)}}{Z_0} \quad t_5 = \frac{\Omega_{-1}^{(1)}}{Z_0} \tag{29}$$

$$\widehat{t}_1 = \frac{1}{2} \qquad \widehat{t}_2 = \frac{1}{2}\,\frac{\rho_0^*(1-\rho_0^*)^{p-2}}{1-(1-\rho_0^*)^{p-1}} \tag{30}$$

where we used the shorthands

$$Z_{+,0,-} \equiv \sum_{\substack{\{q_i\} \\ \sum q_i > 0,\, =0,\, <0}} \prod_{i=1}^{l-1} \widehat{\rho}_{q_i}^* \exp\left\{-\mu_1 \left[\sum_i |q_i| - |\sum_i q_i|\right]\right\}, \tag{31}$$

$$\begin{aligned}\Omega_{\widehat{q}}^{(q)} &\equiv \widehat{\rho}_{\widehat{q}}^* \sum_{\substack{\{q_i\} \\ \sum q_i = q}} \prod_{i=1}^{l-2} \widehat{\rho}_{q_i}^* \cdot \\ &\quad \times \exp\left\{-\mu_1 \left[|\widehat{q}| + \sum_i |q_i| - |\widehat{q} + \sum_i q_i|\right]\right\} \\ &= \widehat{\rho}_{\widehat{q}}^* \exp\left[\mu_1\Big(|\widehat{q}+q| - |\widehat{q}|\Big)\right] \sum_{\substack{\{q_i\} \\ \sum q_i = q}} \prod_{i=1}^{l-2} \widehat{\rho}_{q_i}^*\, \mathrm{e}^{-\mu_1 |q_i|}.\end{aligned} \tag{32}$$

Let us finally notice that the $+/-$ symmetry can be exploited to reduce the matrices (28) to 3×3 matrices, whose product can be write in the following form

$$T \cdot \widehat{T} = \begin{bmatrix} t_1\widehat{t}_1 & 0 & 0 \\ 0 & t_1\widehat{t}_1 & t_3\widehat{t}_2 \\ 0 & t_5\widehat{t}_1 & t_4\widehat{t}_2 \end{bmatrix}. \tag{33}$$

The upper left element corresponds to "large" fluctuations, $\langle\epsilon_-\rangle_+$ and $\langle\epsilon_+\rangle_-$, which are always contracting. The largest eigenvalue of $T \cdot \widehat{T}$ always comes from the 2×2 matrix, which corresponds to "small" fluctuations: $\langle\epsilon_+\rangle_+ \simeq -\langle\epsilon_0\rangle_+$, $\langle\epsilon_+\rangle_0$, $\langle\epsilon_-\rangle_0$ and $\langle\epsilon_-\rangle_- \simeq -\langle\epsilon_0\rangle_-$.

References

1. A. Crisanti, H.-J. Sommers, Z. Phys. B **87**, 341 (1992)
2. A. Crisanti, H. Horner, H.-J. Sommers, Z. Phys. B **92**, 257 (1993)
3. L.F. Cugliandolo, J. Kurchan, Phys. Rev. Lett. **71**, 173 (1993)
4. J.-P. Bouchaud, L.F. Cugliandolo, J. Kurchan, M. Mézard, in *Spin Glasses and Random Fields*, edited by A.P. Young (World Scientific, Singapore, 1997)
5. T.R. Kirkpatrick, D. Thirumalai, Phys. Rev. B **36**, 5388 (1987)
6. J. Kurchan, G. Parisi, M.A. Virasoro, J. Phys. I France **3**, 1819 (1993)
7. R. Monasson, Phys. Rev. Lett. **75**, 2847 (1995)
8. E. Gardner, Nucl. Phys. B **257 [FS14]**, 747 (1985)
9. D. Gross, M. Mézard, Nucl. Phys. B **240 [FS12]**, 431 (1984)
10. L.F. Cugliandolo, J. Kurchan, J. Phys. A **27**, 5749 (1994)
11. L.F. Cugliandolo, J. Kurchan, Phil. Mag. B **71**, 501 (1995)
12. M. Mezard, G. Parisi, M.A. Virasoro, *Spin Glass Theory and Beyond* (World Scientific, Singapore, 1987)
13. E. Marinari, G. Parisi, F. Ritort, J. Phys. A **27**, 7615 (1994)
14. A. Crisanti, T. Rizzo, Phys. Rev. E **65**, 046137 (2002); A. Crisanti, L. Leuzzi, G. Parisi, J. Phys. A **35**, 481 (2002)
15. A.V. Lopatin, L.B. Ioffe, Phys. Rev. B **66**, 174202 (2002)
16. Theor. Comp. Sci. **265**, Issue 1-2, edited by O. Dubois, R. Monasson, B. Selman, R. Zecchina (2001)
17. R. Monasson, J. Phys. A **31**, 513 (1998)
18. M. Mézard, G. Parisi, Eur. Phys. J. B **20**, 217 (2001)
19. S. Franz, M. Leone, F. Ricci-Tersenghi, R. Zecchina, Phys. Rev. Lett. **87**, 127209 (2001)
20. S. Arora. *The approximability of NP-hard problems*, in *Proceedings of the 30th ACM Symposium on Theory of Computing, pages 337–348, 1998*
21. F. Ricci-Tersenghi, M. Weigt, R. Zecchina, Phys. Rev. E **63**, 026702 (2001)
22. S. Cocco, O. Dubois, J. Mandler, R. Monasson, Phys. Rev. Lett. **90**, 047205 (2003)
23. M. Mézard, F. Ricci-Tersenghi, R. Zecchina, J. Stat. Phys. **111**, 505 (2003)
24. A. Montanari, F. Ricci-Tersenghi, in preparation